

# Neuro-3D: Towards 3D Visual Decoding from EEG Signals

## Supplementary Material

### 001 1. EEG Data Preprocessing

002 In this section, we introduce the details of EEG preprocessing  
 003 pipeline. During data acquisition, static 3D image and dynamic 3D video  
 004 stimuli were preceded by a marker to streamline subsequent data processing.  
 005 The continuous EEG recordings were subsequently preprocessed using MNE [5].  
 006 The data were segmented into fixed-length epochs (1s for static stimuli and  
 007 6s for dynamic stimuli), time-locked to stimulus onset, with baseline correction  
 008 achieved by subtracting the mean signal amplitude during the pre-stimulus  
 009 period. The signals were downsampled from 1000 Hz to 250 Hz, and a  
 010 bandpass filter (0.1–100 Hz) was applied in conjunction with a 50 Hz notch  
 011 filter to mitigate noise. To normalize signal amplitude variability across  
 012 channels, multivariate noise normalization was employed [6]. Consistent  
 013 with established practices [8], two stimulus repetitions were treated as  
 014 independent samples during training to enhance learning, while testing  
 015 involved averaging across four repetitions to improve the signal-to-noise  
 016 ratio, following principles similar to those used in Event-Related Potential  
 017 (ERP) analysis [11].

### 022 2. Evaluation Metrics for Reconstruction Benchmark

024 To assess the quality of the generated outputs, we adopt the N-way, top-K  
 025 metric, a standard approach in 2D image decoding [1, 2, 8]. For 2D image  
 026 evaluation, a pre-trained ImageNet1K classifier is used to classify both the  
 027 generated images and their corresponding ground truth images. Similarly,  
 028 we utilize data from Objaverse [3] to pre-train a PointNet++ model [9].  
 029 To ensure classifier reliability, the network is trained on all Objaverse  
 030 data with category labels, excluding the test set used in our study. The  
 031 point cloud data corresponding to the 3D objects is sourced from [12].  
 032 During evaluation, both the generated point clouds and their corresponding  
 033 ground truth point clouds are classified using the trained network. The  
 034 results are then analyzed to confirm whether the reconstructed object is  
 035 correctly identified within the top K categories among N selected. For  
 036 the efficiency of evaluation, we utilize data from the first five subjects  
 037 to train and evaluate the reconstruction model. Moreover, a distinct feature  
 038 of the diffusion model is its dependence on initialization noise, which can  
 039 influence the generated outputs. We perform five independent inferences  
 040 for each object and compute the average N-way, top-K metric across these  
 041 runs. Additionally, to capture the potential best-case performance, we  
 042 identify the optimal result based on the classifier’s predicted scores across  
 043 the five inferences

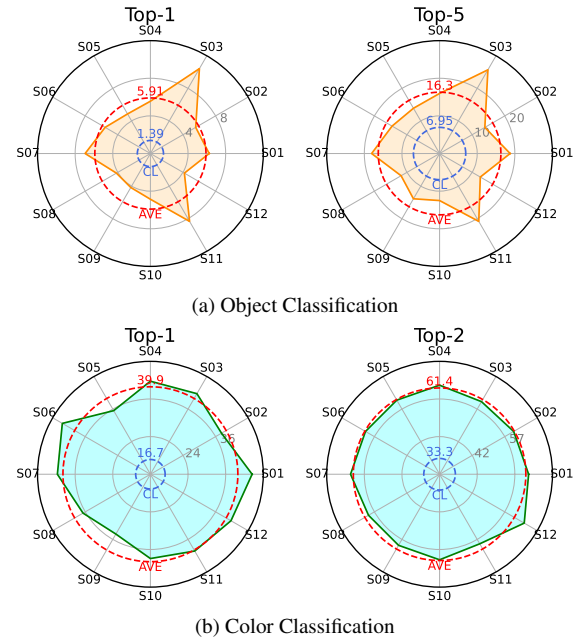


Figure 1. The results of individual analysis. (a) presents the top-1 and top-5 accuracies for the object classification task across 12 subjects, while (b) depicts the top-1 and top-2 accuracies for the classification task. The blue line in each panel indicates chance-level performance, and the red line represents the average performance across all subjects.

and compute the N-way, top-K metric.

### 049 3. Analysis of Individual Difference

050 We present the performance variability across individuals  
 051 on two classification tasks, as illustrated in Fig. 1. On both  
 052 tasks, individual performance consistently exceeds chance  
 053 level, demonstrating that EEG signals encode visual perception  
 054 information and that our method effectively extracts and  
 055 utilizes this information for decoding. Notably, performance  
 056 varies across tasks for the same individual. For instance,  
 057 participant S12 performs significantly below average in object  
 058 classification but achieves above-average results in color  
 059 classification, suggesting distinct neural mechanisms  
 060 underlying the processing of different visual attributes  
 061 and their representation in EEG signals.

062 Furthermore, it has been widely confirmed that EEG signal  
 063 has substantial individual variations [4, 7, 10]. As shown  
 064 in Fig. 1, significant differences are observed between  
 065 individuals performing the same task, particularly in object  
 066 classification, where S03 and S11 exhibit superior performance



Figure 2. More results reconstructed by Neuro-3D with different samplings trials, and the corresponding ground truth. The sampling variations arise either from results obtained across different subjects or from inference outputs of the diffusion model for the same subject using distinct noise initializations.

067 mance, while  $S_{08}$ ,  $S_{09}$  and  $S_{12}$  fall markedly below average. Similar variability is observed in the color classification task, albeit to a lesser extent. These results underscore the pronounced inter-subject differences in EEG signals and highlight a critical challenge for cross-subject EEG visual decoding tasks, where performance remains suboptimal. Addressing this variability is a key direction for future research.

#### 075 4. More Reconstructed Samples

076 Additional reconstructed results alongside their corresponding ground truth point clouds are presented in Fig. 2. The proposed Neuro-3D framework exhibits robust performance, effectively capturing semantic categories, shape details, and the overall color of various objects.

#### 081 5. Analysis of Failure Cases



Figure 3. Failure cases. (a) highlights reconstructions with significant loss of fine details, while (b) demonstrates several instances of incorrect semantic category prediction.

082 Fig. 3 illustrates representative failure cases, categorized  
 083 into two principal types: inaccuracies in detailed shape pre-  
 084 diction and semantic reconstruction errors. Despite these  
 085 limitations, certain features of the stimulus objects, includ-  
 086 ing shape contours and color information, are partially pre-  
 087 served in the displayed reconstructed images. These short-  
 088 comings primarily arise from the inherent challenges of the  
 089 low signal-to-noise ratio and limited spatial resolution of  
 090 EEG signals, which constrain the performance of 3D object  
 091 reconstruction. Addressing these issues presents a promis-  
 092 ing direction for future improvement.

## References

- [1] Zijiao Chen, Jiaxin Qing, Tiange Xiang, Wan Lin Yue, and Juan Helen Zhou. Seeing beyond the brain: Masked modeling conditioned diffusion model for human vision decoding. In *Proceedings of the IEEE/CVF Conference on Computer Vision and Pattern Recognition*, 2023. 1
- [2] Zijiao Chen, Jiaxin Qing, and Juan Helen Zhou. Cinematic mindscapes: High-quality video reconstruction from brain activity. *Advances in Neural Information Processing Systems*, 36, 2024. 1
- [3] Matt Deitke, Dustin Schwenk, Jordi Salvador, Luca Weihs, Oscar Michel, Eli VanderBilt, Ludwig Schmidt, Kiana Ehsani, Aniruddha Kembhavi, and Ali Farhadi. Objaverse: A universe of annotated 3D objects. In *Proceedings of the IEEE/CVF Conference on Computer Vision and Pattern Recognition*, pages 13142–13153, 2023. 1
- [4] Erin Gibson, Nancy J Lobaugh, Steve Joordens, and Anthony R McIntosh. Eeg variability: Task-driven or subject-driven signal of interest? *NeuroImage*, 252:119034, 2022. 1
- [5] Alexandre Gramfort, Martin Luessi, Eric Larson, Denis A Engemann, Daniel Strohmeier, Christian Brodbeck, Roman Goj, Mainak Jas, Teon Brooks, Lauri Parkkonen, et al. MEG and EEG data analysis with MNE-Python. *Frontiers in Neuroinformatics*, 7:267, 2013. 1
- [6] Matthias Guggenmos, Philipp Sterzer, and Radoslaw Martin Cichy. Multivariate pattern analysis for meg: A comparison of dissimilarity measures. *NeuroImage*, 173:434–447, 2018. 1
- [7] Gan Huang, Zhiheng Zhao, Shaorong Zhang, Zhenxing Hu, Jiaming Fan, Meisong Fu, Jiale Chen, Yaqiong Xiao, Jun Wang, and Guo Dan. Discrepancy between inter-and intra-subject variability in eeg-based motor imagery brain-computer interface: Evidence from multiple perspectives. *Frontiers in Neuroscience*, 17:1122661, 2023. 1
- [8] Dongyang Li, Chen Wei, Shiyong Li, Jiachen Zou, and Quanying Liu. Visual decoding and reconstruction via EEG embeddings with guided diffusion. In *Advances in Neural Information Processing Systems*, 2024. 1
- [9] Charles Ruizhongtai Qi, Li Yi, Hao Su, and Leonidas J Guibas. Pointnet++: Deep hierarchical feature learning on point sets in a metric space. *Advances in Neural Information Processing Systems*, 30, 2017. 1
- [10] Simanto Saha and Mathias Baumert. Intra-and inter-subject variability in eeg-based sensorimotor brain computer interface: a review. *Frontiers in Computational Neuroscience*, 13:87, 2020. 1
- [11] Shravani Sur and Vinod Kumar Sinha. Event-related potential: An overview. *Industrial Psychiatry Journal*, 18(1):70–73, 2009. 1
- [12] Runsen Xu, Xiaolong Wang, Tai Wang, Yilun Chen, Jiangmiao Pang, and Dahua Lin. Pointllm: Empowering large language models to understand point clouds. *European Conference on Computer Vision*, 2024. 1